

## Research paper

# Continuous wet granulation using fluidized-bed techniques I. Examination of powder mixing kinetics and preliminary granulation experiments

Silke Gotthardt<sup>a,b</sup>, Axel Knoch<sup>b</sup>, Geoffrey Lee<sup>a,\*</sup><sup>a</sup>*Department of Pharmaceutical Technology, Friedrich-Alexander-University, Erlangen, Germany*<sup>b</sup>*Parke-Davis GmbH, Freiburg, Germany*

Received 19 January 1999; accepted in revised form 6 July 1999

---

## Abstract

The movement of powder/granules within the reaction chambers of two continuously-operating granulators (Niro/Aeromatic-Fielder Contipharm and the Glatt Continuous Fluidized-Bed Granulator) was examined by adding dyestuffs to the powder-inlet. Comparison of the dye mass-fraction in the product with the appropriate transport equation indicated random mixing and transport within the product-chamber. Photographs of powder movement on the gill-plate of the Contipharm showed, however, air-driven transport of powder from inlet to outlet, which evidently does not prevent overall random mixing. The output half-life is >20 min, showing substantial residence time within each machine. A simplex granule was also prepared using the two machines. With the Niro it was shown that an increase in binder solution spraying rate during the continuous process produced an increase in particle size distribution and moisture content. Reduction of air volumetric flow rate on the Glatt machine during continuous operation produced higher moisture content of the product. It was thus demonstrated that changes in process conditions during continuous operation produce predictable alterations in product properties. © 1999 Elsevier Science B.V. All rights reserved.

**Keywords:** Continuous granulation; Kinetics

---

## 1. Introduction

Granulation within the pharmaceutical industry is a batch process. All the conventional machines for wet granulation, for example high shear mixers or fluidized-bed units, can only be operated in a batch-wise manner. Continuous granulation has, however, some important advantages. It reduces the number of process steps [1], and material handling is simplified since less time is required for filling, emptying and cleaning machines [2]. Additionally, the ‘batch’ size is determined by the running time of the machine, and not by its volume capacity [3]. It suffers, however, from two limitations to its application within pharmacy. First, product uniformity necessitates exact continuous dosing of both powder and granulation liquid [4], placing strenuous demands on transport equipment and pumps. Secondly, a continuous process produces large quantities of a single product [5], whereas in pharmaceutical production numerous small-volume products are manufactured. A further

complication arises from the absence of a clearly-defined batch during continuous production. This problem is overcome by using the alternative nomenclature ‘batch continuous’ [6], where the batch is defined as the amount of product manufactured within one 24-h period or one working shift [7].

The literature of the last 20 years contains a number of references to continuously operating mixer granulators and fluidized-bed granulators, reviewed in detail elsewhere [4,8]. They all have serious disadvantages. Quasi-continuous granulators [9] combine mixer, sift granulator and fluidized-bed dryer in serial combination. They require exact co-ordination of the working speeds of the individual units relative to one another, rendering operation complicated and time consuming, with numerous interruptions caused by readjustment of the individual units. ‘Single cell’ fluidized-bed granulators operate with simultaneous mixing, agglomeration and drying [10], although this is difficult to achieve because of the different process conditions, viz. temperature and moisture level, required for each of these steps. This problem can be overcome using ‘multi-cell’ fluidized-bed granulators [11], comprising a horizontal processing chamber divided by doors into a number of segments. The doors can be opened or closed according to the current

---

\* Corresponding author. Lehrstuhl für Pharmazeutische Technologie, Cauerstrasse 4, D-91058 Erlangen, Germany. Tel.: +49-9131-852-9552; fax: +49-9131-852-9545.

E-mail address: lee@pharmtech.uni-erlangen.de (G. Lee)

stage of the granulation process. Construction is therefore complicated, and the process suffers inevitably from the same problem of poor co-ordination of the serially-running processes of mixing, agglomeration, and drying [12]. It is therefore not surprising that none of these machines has found acceptance within the pharmaceutical industry.

Recently, two new continuously-operating fluidized-bed granulators designed to avoid the problems described above have been developed. The Contipharm from Niro/Aeromatic-Fielder is a fluidized-bed production machine suitable for work at GMP standards [13]. The Fluidized-Bed Granulator from Glatt is a pilot unit, developed for trials of continuous granulation. They are both single-cell machines, whose processing chambers although partly divided into regions have, however, no doors. Mixing, agglomeration and drying are claimed to occur sequentially as the product passes through the chamber. In this paper we address the question of movement of powder and aggregates within the reaction chambers of the two machines. An experiment was conceived and a kinetic model developed to examine this process and judge if the 'single-cell' construction produces directional transport or random mixing within the reaction chamber. To determine the relevance of our findings for the practical use of these machines we also undertook two preliminary experiments to examine how changes in spraying rate (with the Contipharm) and air volumetric flow rate (Glatt) effect product properties. No attempt was made to optimize the conditions, this being outside the scope of the brief study made here. Taken together, the results presented in this paper illustrate the strengths and limitations of both machines.

## 2. The continuously-operating fluidized-bed granulators

### 2.1. Niro/Aeromatic-Fielder Contipharm (Niro granulator)

As illustrated in Fig. 1a, the granulator is divided by a sieve floor (6) horizontally into two chambers. The lower inlet-air chamber (7) is of multi-cell design and divided into three zones by two vertical walls. The air passes upwards through the sieve floor (6) into the overlying reaction chamber (5) which has no vertical walls and is therefore of single-cell design. The sieve floor has the gill-plate construction illustrated in Fig. 1b, intended [14,15] to produce directional transport of the reaction chamber's contents from the powder inlet (1) to the product outlet (2). Spray nozzles are attached to the sieve floor in bottom-spray fashion. The top of the reaction chamber is formed by two parallel rows of eight sintered-metal filters (4), each of area  $0.56 \text{ m}^2$ .

The inlet-air temperature and volumetric flow rate can be separately specified in each of the three zones of the inlet-air chamber. Thus, in the overlying reaction chamber the spatially-varying conditions for mixing, agglomeration and drying can be selected (and optimized, although not done here). This is intended to avoid the problems of the

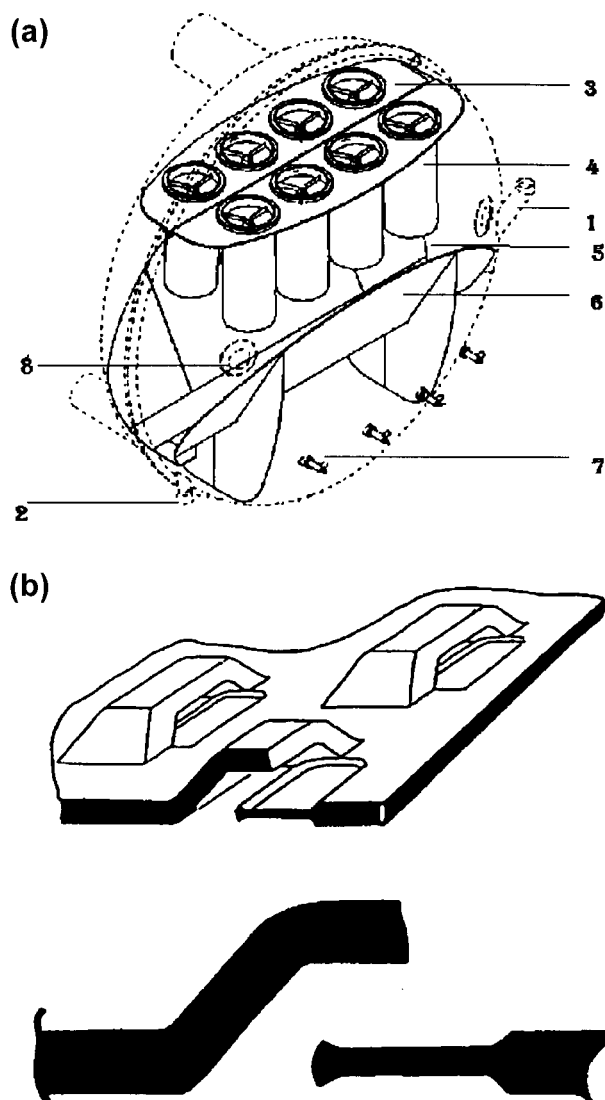


Fig. 1. (a) Reaction chamber of Niro granulator. (1) Powder inlet; (2) product outlet; (3) filter outlet; (4) filters; (5) reaction chamber; (6) sieve floor; (7) inlet-air chamber; (8) inspection window. (b) Detail of gill-plate forming sieve floor from Niro granulator.

earlier single-cell [10] and multi-cell [11] fluidized-bed granulators. The intended material transport within the reaction chamber [14] is as follows. The powder enters into the first region of the reaction chamber where it is mixed. Passing onwards, the granulation liquid is sprayed onto the powder and agglomeration occurs. Passing further, the granules are dried and finally transported out of the reaction chamber. The gill-plate sieve floor is intended to guarantee this directional transport of powder through the reaction chamber [14,15].

### 2.2. Glatt Continuous Fluidized-Bed Granulator (Glatt granulator)

This machine also has two horizontal chambers, the

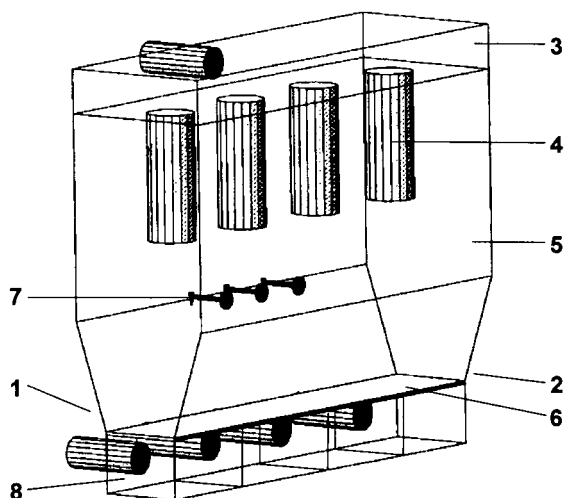


Fig. 2. Reaction chamber of Glatt granulator. (1) Powder inlet; (2) product outlet; (3) filter outlet; (4) filters; (5) reaction chamber; (6) sieve floor; (7) spray nozzle; (8) inlet air chamber.

inlet-air chamber (8) and the reaction chamber (5) (Fig. 2). The inlet-air chamber is divided by three vertical walls into four zones, in each of which the temperature and air volumetric flow rate is separately controllable. The major difference to the Niro granulator is, however, the construction of the sieve floor (6) separating the inlet-air and overlying reaction chambers. It has uniformly placed round perforations having a total cross-sectional area of approx. 12% of the floor, and is not therefore specifically designed to produce directional powder transport. The top of the reaction chamber is formed by four metal filters (4), each of 0.46 m<sup>2</sup> area.

The divisions of the inlet-air chamber produce 4 regions of differing process conditions within the reaction chamber. They are intended to function as follows. Following mixing within the first region, the powder is agglomerated within the second and third regions by top-spray (Fig. 2), and dried within the fourth region. No information is available regarding transport through the reaction chamber of this machine.

### 3. Material and methods

A simplex granule was prepared from 8 parts Lactose D20 (Capsulac60, Meggle GmbH, Wasserburg, Germany) and 2 parts maize starch (TypeB, Roquette GmbH, Frankfurt, Germany). The two components were premixed in a container mixer (Engelsmann AG, Ludwigshafen, Germany) for 20 min at 8 rev./min. The granulating liquid was a 5% w/w aqueous PVP solution (PVP K29, ISP, Frechen, Germany). To examine the material transport within the reaction chambers, Methylene Blue and Sudan III Red (both Merck, Darmstadt, Germany) were used.

#### 3.1. Investigation of material transport within reaction chambers

Both machines were initially run-up in batch mode before being changed to continuous operation. The reaction chamber of each granulator was initially filled with the powder mixture (50 kg in the Niro machine and 45 kg in the Glatt machine, determined by machine design and capacity) and granulated in batch mode by spraying 20 l of the PVP solution at an inlet-air temperature of 80°C and volumetric flow rate of 600 m<sup>3</sup>/h in all zones. After 1 h, the machine was changed to continuous mode by opening the powder inlet and product outlet, and setting the powder inlet feed rate to 1 kg/min. The granulation liquid was sprayed at 0.44 l/min. With the Niro machine the drying-air temperatures and volumetric flow rates were 80°C/200 m<sup>3</sup>/h (mixing zone), 80°C/600 m<sup>3</sup>/h (agglomeration zone) and 105°C/200 m<sup>3</sup>/h (drying zone). With the Glatt machine the conditions were 100°C/350 m<sup>3</sup>/h in all four zones [14]. The different conditions for the two machines reflect their different construction and are recommended values cited by the manufacturers.

The transport kinetics of powder/granules through the reaction chamber of each machine was then examined by adding 10 g of either Methylene Blue or Sudan III Red to the immediate vicinity of the powder inlet. The resulting dye content of the product granules (mass fraction of dye, mg/g) was determined by taking 20 g samples at the product outlet over 95 min and determining their dye content photometrically. The samples were dissolved or suspended in water (Methylene Blue) or hexane (Sudan III Red), and after centrifugation the optical density of clear supernatant was measured at  $\lambda = 664$  nm for Methylene Blue or  $\lambda = 498$  nm for Sudan III Red. The calibration curves for the dyes were obtained using physical mixtures of the granules and dyes.

The movement of powder across the gill-plate of the Niro granulator was examined visually by placing an isolated section of the plate on a laboratory fluidized-bed dryer (Strea, Aeromatic-Fielder) having a plexiglass cover (Fig. 3). 200 g lactose was layered on to the left side of the gill-plate, and this side fluidized uniformly from below. The right side of the gill-plate was not exposed to inlet air (see Fig. 3). Photographs of powder movement were taken using a still-frame camera.

#### 3.2. Granulation experiments

Two granulation experiments were performed to determine how the two machines react to change in process conditions (spray rate on the Niro and air temperature on the Glatt) during continuous operation. These were designed as preliminary experiments, to complement the results of measurement of material transport through the two machines. No attempt was made to optimize the granulation conditions.

Both machines were again initially run-up in batch mode before being changed to continuous operation. The 50 kg of

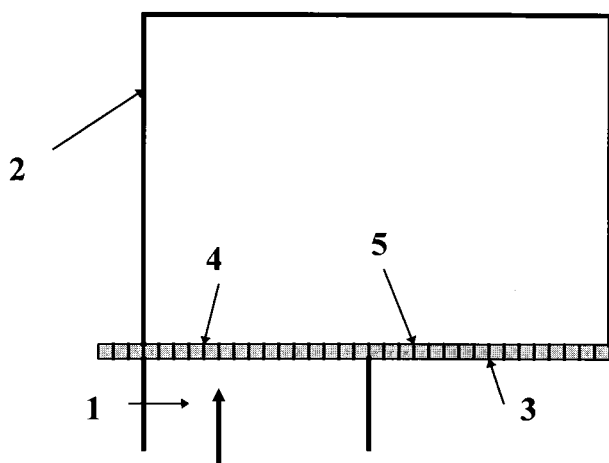


Fig. 3. Fluidized-bed apparatus used to examine powder transport across gill-plate of Niro granulator. (1) Air inlet; (2) plexiglass cover; (3) gill-plate; (4) fluidized left-hand-side; (5) non-fluidized right-hand-side.

powder in the Niro granulator was granulated in batch mode by spraying with 16.5 l of the PVP solution at an inlet-air temperature of 80°C. These conditions were selected intuitively to give approx. 1.5% binder content in the granules. After 1 h pre-granulation, the machine was changed to continuous mode by opening the powder inlet and the product outlet, and setting the powder inlet feed rate to 1 kg/min. The granulation liquid was sprayed at 0.33 l/min with air temperatures and volumetric flow rates of 80°C/200 m<sup>3</sup>/h (mixing zone), 80°C/600 m<sup>3</sup>/h (agglomeration zone) and 95°C/200 m<sup>3</sup>/h (drying zone). The conditions were again selected from recommendations of the manufacturer. After 2 h continuous operation the spray rate was increased to 0.4 l/min and the air temperature in the drying zone increased to 105°C. At various time intervals, samples of 20 g were removed at the product outlet running on a moving band, and were analysed as given below.

In a similar fashion the Glatt granulator was initially run for 1 h in batch mode after loading with 45 kg of powder. This was sprayed with 20 l of the PVP solution to give a higher binder content of the granules than with the Niro machine (see Section 4). The granules were dried at 90°C (because of the higher spraying rate), before changing to continuous mode at a powder inlet rate of 1 kg/min. The granulation liquid was sprayed at 0.4 l/min to maintain the higher binder content of the product. The inlet-air temperature was kept constant at 100°C in all four zones, whereas the air volumetric flow rate was reduced stepwise in all four zones according to the pattern shown in Fig. 4. At regular times, samples of 20 g were taken at the product outlet and analysed as given below.

### 3.3. Granule properties

The moisture content of the granules was determined gravimetrically using a Mettler IR dryer (Mettler AG, Greifensee, Switzerland). Sieve analysis was performed on a

Vibrotonic VE1 Sieve Tower (Retsch, Hahn, Germany). 100 g of granule was shaken for 10 min at an amplitude of 1.5 mm, after which the residue on each sieve was weighed.

## 4. Results and discussion

### 4.1. Material transport within product chamber of machines

The change in mass-fraction of dye (mg/g) in the samples drawn from the product outlet with time is shown in Fig. 5a. With the Niro granulator, the water-soluble Methylene Blue is detectable at the product outlet in the first sample drawn 5 min after adding the dye to the powder inlet. The dye mass-fraction then increases rapidly with time and reaches a maximum after  $t_{max} = 12.5$  min, after which it decreases in an apparently negative exponential fashion. The mass-fractions of Methylene Blue and the water-insoluble Sudan III-Red with the Glatt granulator are higher at 5 min, and have slightly larger values for  $t_{max}$  (17.5 min for Methylene Blue and 15 min for Sudan III Red). It follows that the water solubility of Methylene Blue is not responsible for the tailing-off in mass-fraction after  $t_{max}$ , since the same effect is seen with the water-insoluble Sudan III Red.

To interpret these results in terms of mixing of powder (p) and dye (d) within the reaction chamber of each machine we assume sequential first-order processes for the entrance and exit of the dye into/from the reaction chamber. A known mass of dye is added to the powder inlet feed of the continuously-operating reaction chamber, whilst the resulting dye mass-fraction in the granules emerging from the product outlet is measured. To describe this process mathematically, two chambers are required (Fig. 6): the granulator's reaction chamber, in which spontaneous mixing of the powder mass,  $m_p(t)$ , and dye mass,  $m_d(t)$ , is specified; and the fictitious pre-chamber, which allows description of the introduction of a mass of dye into the continuous feed of the reaction cham-

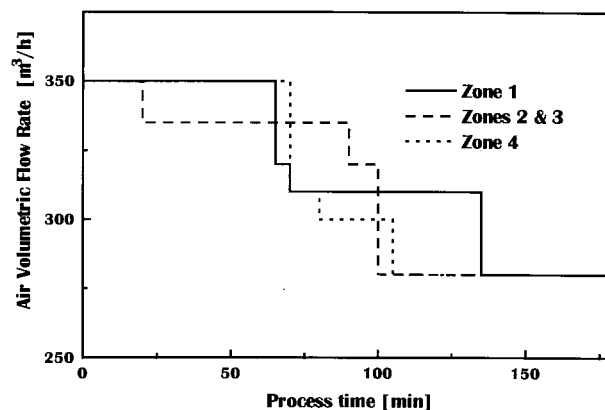


Fig. 4. Change in drying air rate during continuous mode with the Glatt granulator. The initial air rate of 350 m<sup>3</sup>/h was progressively reduced in the four zones.

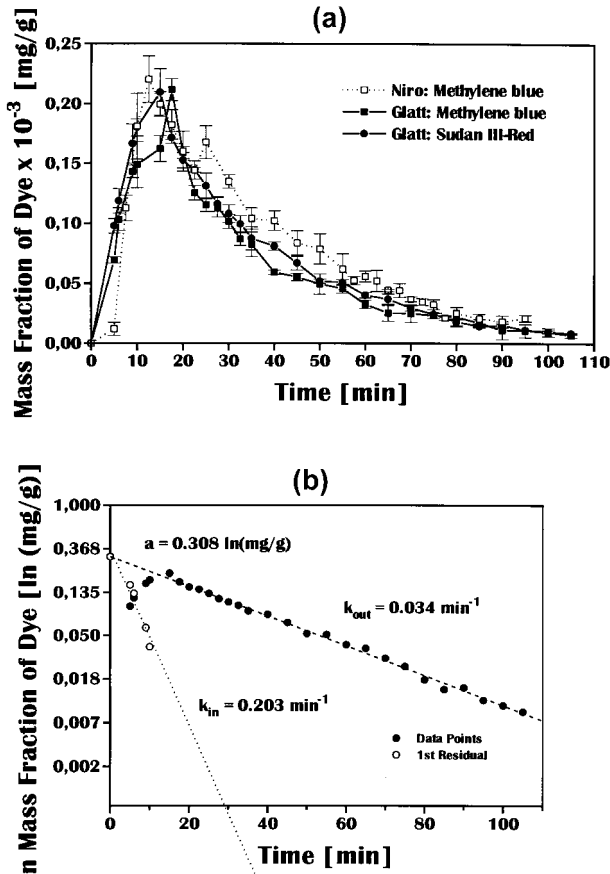


Fig. 5. (a) Change in mass-fraction of dye in product granules (mg/g) with time after introduction of 10 g dye into powder inlet.  $n = 4$ . (b) Example plot of Eq. (8) with  $\Phi_d(t)$ -data obtained for Sudan III Red with Glatt granulator. The slope for  $k_{in}$  was obtained using the method of residues.

ber. The pre-chamber is initially loaded with a mixture of powder of mass  $m_p^*(t)$  and dye of mass  $m_d^*(t)$ . The latter represents the 10 g of dye added to the powder inlet in this experiment. This powder/dye mixture in the pre-chamber is transported at  $t > 0$  with zero-order kinetics of rate  $k_{in}^*$  (1 kg/min) into the reaction chamber, the content mass of the pre-chamber being kept constant by adding powder. The reaction chamber initially contains no dye ( $t = 0$ ), and its contents are transported at  $t > 0$  with zero-order kinetics of rate  $k_{out}$  (1 kg/min) through the inlet. As soon as the complete contents of the pre-chamber have been emptied into the reaction chamber at  $t = t_{dye}$ , further input of pure powder at  $k_{in} = 1 \text{ kg/min}$  occurs until the end of the experiment. Thus the total mass of powder plus dye which enters or leaves the reaction chamber is given by zero order kinetics. The mass of dye which enters or leaves the reaction chamber is, however, given by first-order kinetics as follows.

The mass-fraction of dye in the pre-chamber is given by:

$$\Phi_d^*(t) = m_d^*(t)/m_0^* \quad (1)$$

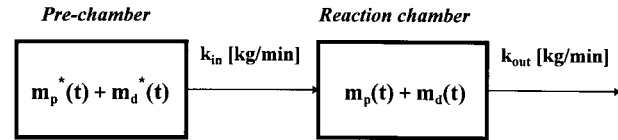


Fig. 6. Model representing introduction of dye into powder inlet of reaction chamber. See text for explanation and detail.

where  $m_0^*$  is the fictitious total mass of the contents of the pre-chamber:

$$m_0^* = m_d^*(t) + m_p^*(t)$$

= const. (2) The decrease in  $\Phi_d^*(t)$  with time caused by the dye/powder mixture moving into the reaction chamber whilst keeping  $m_0^*$  constant is then a first-order process:

$$\frac{-d\Phi_d^*(t)}{dt} = k_{in} \frac{\Phi_d^*(t)}{m_0^*} \quad (3)$$

whose solution is:

$$\Phi_d^*(t) = \Phi_d^*(0) e^{-\frac{k_{in}}{m_0^*} t} \quad (4)$$

Eq. (4) thus describes the mass-fraction of dye in the powder being fed via the inlet into the reaction chamber at any time during the experiment. The resulting mass fraction of dye within the reaction chamber is defined in a similar way as:

$$\Phi_d(t) = m_d(t)/m_0 \quad (5)$$

where

$$m_0 = m_d(t) + m_p(t) = \text{const.} \quad (6)$$

The change in  $\Phi_d(t)$  with time is:

$$\frac{-d\Phi_d(t)}{dt} = k_{out} \frac{\Phi_d(t)}{m_0} - k_{in} \frac{\Phi_d^*(t)}{m_0} \quad (7)$$

Thus the mass of dye leaving the reaction chamber is also a first-order process. Substituting from Eq. (4) yields:

$$\frac{-d\Phi_d(t)}{dt} = k_{out} \frac{\Phi_d(t)}{m_0} - k_{in} \frac{\Phi_d^*(0)}{m_0} e^{-\frac{k_{in}}{m_0^*} t} \quad (8)$$

This is the familiar Bateman ordinary differential equation of first order with constant coefficients, whose solution is:

$$\Phi_d(t) = \frac{k_{in} m_d^*(0)}{k_{in} m_0 - k_{out} m_0^*} \left( e^{-\frac{k_{out}}{m_0} t} - e^{-\frac{k_{in}}{m_0^*} t} \right) \quad (9)$$

since  $k_{in}/m_0^* > k_{out}/m_0$ .  $\Phi_d(t)$  is the mass fraction of dye in the product emerging from the outlet,  $k_{in}$  and  $k_{out}$  are the rates of inlet feed and product outlet,  $m_d^*(0)$  is the mass of dye introduced into the inlet, and  $m_0$  is the total powder capacity of the reaction chamber. Fig. 5b shows the best fit of the Eq. (9) to the semi-logarithmic plot of the  $\Phi_d(t)$  versus  $t$  data for the example of Sudan III Red in the Glatt granulator. It is evident that the  $\Phi_d(t)$  values fit the predicted logarithmic dye output from the reaction chamber after  $t_{dye}$

Table 1  
Fitted parameters of Eq. (1) for the  $\Phi_d(t)$  versus  $t$  data

Machine	Dye	$k_{out}/m_0$ (l/min)	$m_0$ (kg)	$k_{in}/m_0^*$ (l/min)	$m_0^*$ (kg)	Intercept on y-axis (ln(g/g))	$m_d^*(0)$ (g)
Glatt	Sudan Red	0.034	29	0.203	4.9	$3.08 \times 10^{-4}$	7.4
Glatt	Meth. Blue	0.035	29	0.204	4.9	$2.91 \times 10^{-4}$	7.0
Niro	Meth. Blue	0.032	31	0.210	4.7	$3.35 \times 10^{-4}$	8.1

very well. The fitted model parameters from all three experiments are shown in Table 1. The first-order input parameter,  $k_{in}/m_0^*$ , has units 1/time and shows that approx. 20% of the dye mass enters the reaction chamber per minute giving an input half-life of approx. 3.5 min. If a first-order process is effectively complete after 5 half-lives, the total dye mass has entered the reaction chamber after approx. 17.5 min. The points of inflexion in the downward curves on Fig. 5a lie therefore between 15 and 20 min, at which time input of the dye with the powder is complete. The first-order outlet parameter,  $k_{out}/m_0$ , of approx.  $0.033 \times 1/\text{min}$  (Table 1) yields an output half-life of 21 min. The fitted values for  $m_0$  and  $m_d^*(0)$  (Table 1) are approx. 30 kg and 7–8 g, respectively, compared with their time values of  $m_0 = 50$  kg (Niro) or 45 kg (Glatt) and  $m_d^*(0) = 10$ g. The differences between fitted and real values for these parameters are not surprising considering the inevitable fluctuations in input and output of the machines, and hence in  $m_0$ . Despite these deviations, Eq. (9) gives a workable description of the input/mixing/output of the dyes in the reaction chambers of the two continuous granulators. As with any compartment model the assumption is made that the dye mass-fraction within the reaction chamber is space-independent and purely a function of  $t$ . This indicates random mixing of dye and powder within the reaction chamber and no directional powder transport. Interestingly, the same results are obtained for both granulators. The Glatt machine has a regular sieve-plate floor of the reaction chamber, and random mixing in the fluidized bed is to be expected. The Niro machine has, however, the gill-plate floor, which is supposed to produce directional movement of its contents from inlet to exit.

#### 4.2. Powder movement on Niro gill-plate

Fig. 7a–c illustrate in time-sequence how powder is rapidly directionally-transported over the gill-plate from left to right. Within this closed experimental set-up (cf. Fig. 3, no air-outlet on top, no material inlet or outlet) the right wall of the plexiglass cover prevents further lateral movement of the powder, which is blown upwards, falling back into the left-hand side of the chamber. On turning off the fluidizing air, the powder pattern on the gill-plate (Fig. 7d) illustrates how the air inlets on the gill-plate (cf. Fig. 1b) produce air-flow driven transport of powder from left to right across the plate.

The different geometry of the experimental set-up compared with the reaction chamber of the Niro granulator

prohibits a direct comparison of powder movement. The rapid air-driven flow of powder across the gill-plate must, however, be viewed in terms of the output half-life of 21 min calculated from the  $\Phi_d(t)$ -data in Fig. 5b. There must be substantial circulation of powder within the reaction-chamber that causes its retention there. In this case, Fig. 5b indicates that the gill-plate floor of the Niro granulator has no apparent advantage in this regard over the regular perforated floor of the Glatt granulator. In both cases powder is maintained within the reaction chamber for a much longer time than necessary to transport it directly from inlet to outlet.

#### 4.3. Granulation in Niro granulator

Sieve analysis of the lactose/starch powder mixture fed into the granulators gave a log-normal size distribution (not shown), with a geometric mean diameter,  $d_g$ , of 216  $\mu\text{m}$  and a geometric standard deviation,  $\sigma_g$ , of 1.302. The fines content (defined as  $d < 180 \mu\text{m}$ ) was 33% w/w.

The initial pre-granulation step in batch mode is equivalent to a conventional granulation process [15] and gave granules containing 2.3% w/w moisture (Fig. 8a). This low value is a result of the long drying treatment (1 h at 80°C). During this pre-granulation step there was evidently no particle aggregation, since  $d_g$  (Fig. 8b) and  $\sigma_g$  (Fig. 8c) are not different to those of the original powder mixture, owing to insufficient binder. The change to continuous mode at a spraying rate of 0.33 l/min produces an increase in  $d_g$  (Fig. 8b) and a decrease in  $\sigma_g$  (Fig. 8c). The change in  $d_g$  is, however, so small that it can only represent binding of the fines to the larger particles. This would explain the reduction in  $\sigma_g$  in the first minutes of continuous operation. After some 30 min in continuous mode both  $d_g$  and  $\sigma_g$  have stabilized, and the product contains approx. 3% w/w moisture (Fig. 8a).

In a conventional batch process the problem of insufficient binder would necessitate a second experiment. With the continuous process, however, the spraying rate could be increased at will, in this case to 0.40 l/min after 120 min. When measured again at 210 min,  $d_g$  has increased to approx. 250  $\mu\text{m}$ , with a slight reduction in  $\sigma_g$  to below 1.3 (Figs. 8b,c). Since the drying air temperature and volumetric flow rate remained unchanged, the product also shows a higher moisture content of approx. 4% w/w (Fig. 8a). Clearly, the PVP content is still insufficient to yield satisfactory agglomeration. No attempt was made to optimize the binder content via the spraying rate, since we were only

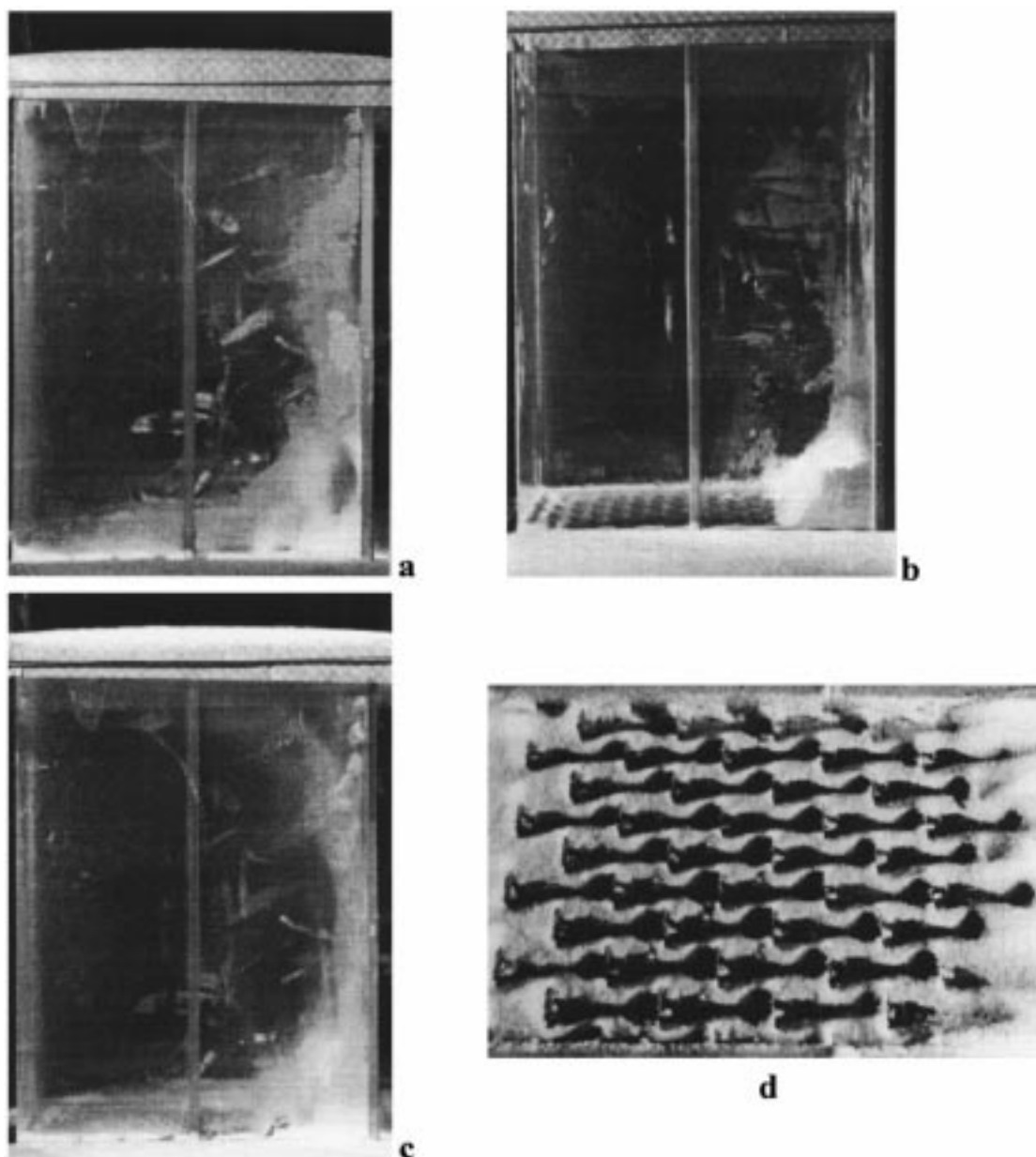


Fig. 7. Powder movement on gill-plate with plexiglass cover. The left side of the base is comprised of the gill-plate served with fluidizing air, whilst the right side has a solid base. (a–c) Directional movement of powder across gill-plate. (d) Powder pattern on gill-plate at conclusion of experiment.

interested in demonstrating that a change in process conditions during continuous operation modifies product properties in a predictable way.

#### 4.4. Granulation in Glatt granulator

The Glatt granulator was also run for the first 1 h in batch mode as a pre-granulation step, but using more binder solution (20 l on 45 kg powder, instead of 16 l on 50 kg). The moisture content of these granules is 1% w/w (Fig. 9a), as a consequence of the higher drying-air temperature of 90°C compared with 80°C for the Niro granulator. The higher PVP content produces a slightly higher  $d_g$  of 285  $\mu\text{m}$  at

the end of batch mode (Fig. 9b), with a wide  $\sigma_g$  of 1.43 (Fig. 9c).

On changing to continuous mode, the binder solution spraying rate was increased to 0.44 l/min, compared with 0.4 l/min at the end of the Niro experiment. With the Glatt machine the influence of air volumetric flow rate was examined, which was reduced stepwise in all four sections of the chamber over a total granulating time of 3 h. During the first 20 min under an air volumetric flow rate of 350  $\text{m}^3/\text{h}$  in all four zones was used (cf. Fig. 4) and the granule moisture remains at the low level of approx. 1% w/w seen in pre-granulation (Fig. 9a).  $d_g$  increases, however, up to 330  $\mu\text{m}$  (Fig. 9b) whilst  $\sigma_g$  remains unchanged (Fig. 9c). At this

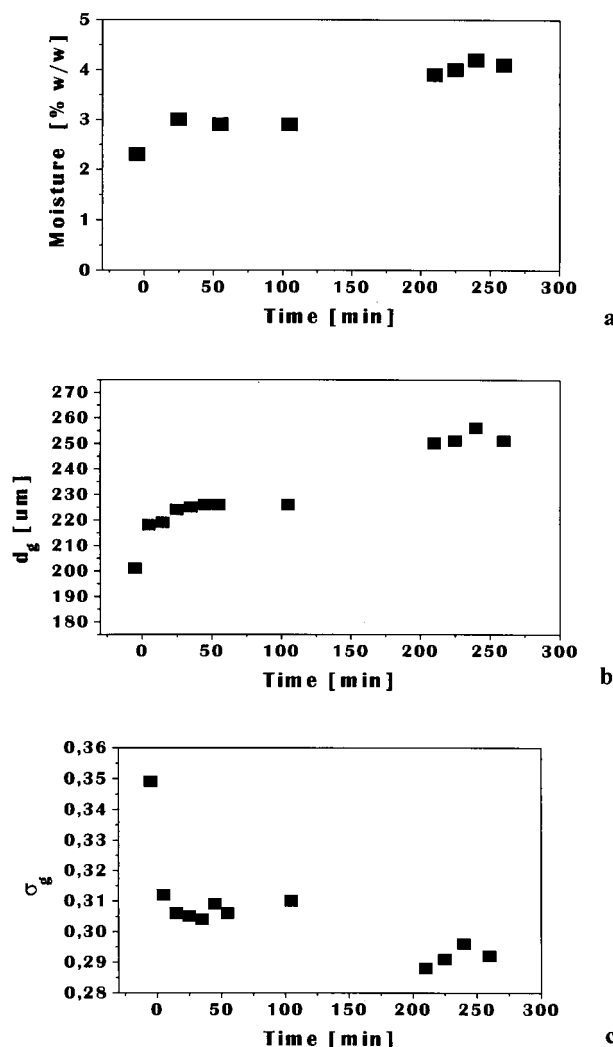


Fig. 8. Product properties produced with the Niro granulator. (a) Residual moisture; (b) geometric mean diameter; (c) geometric standard deviation. Operation:  $t < 0$ , pre-granulation in batch mode;  $t = 0$ , change to continuous mode;  $t = 120$ , increase in spray rate from 0.33 to 0.4 l/min.

point ( $t = 20$  min) the air volumetric flow rate in the granulation zones (2 and 3) was reduced from 350 to 330  $\text{m}^3/\text{h}$ , causing an increase in product moisture content to approx. 1.2% w/w (Fig. 9a) because of reduced drying rate. The steady increase in  $d_g$  seen after the change to continuous operation continues, and it stabilises only after 1 h at approx. 360  $\mu\text{m}$  (Fig. 9b). The increase in binder spraying rate produces therefore more particle agglomeration, although still only moderate. The subsequent ( $t \geq 90$  min) stepwise reductions in air volumetric flow rate to 280  $\text{m}^3/\text{h}$  in all four zones (cf. Fig. 4) produce no substantial further change in product moisture content (Fig. 9a),  $d_g$  (Fig. 9b) or  $\sigma_g$  (Fig. 9c). Thus change in air volumetric flow rate during continuous operation also produces predictable alterations in product properties. As with the Niro machine, no attempt was made to optimize the process; we just wished to demonstrate this point. Despite the reduction in air volumetric flow

rate at  $t = 20$  min, it is evident from the  $d_g$  and  $\sigma_g$  data that the Glatt granulator also takes  $>30$  min to yield a stable product after the change from batch to continuous mode.

## 5. Conclusions

Although the kinetic model represents only a simplification of material movement into and out of the two continuous granulators, it provides evidence of random mixing within the reaction chambers of differing construction. This occurs in the Glatt machine despite the visual evidence of air-driven directional transport across the gill-plate. The values obtained for input and output half-lives (3.5 and 21 min, respectively) illustrate the complex nature of the material transport. With both granulators it was possible to alter

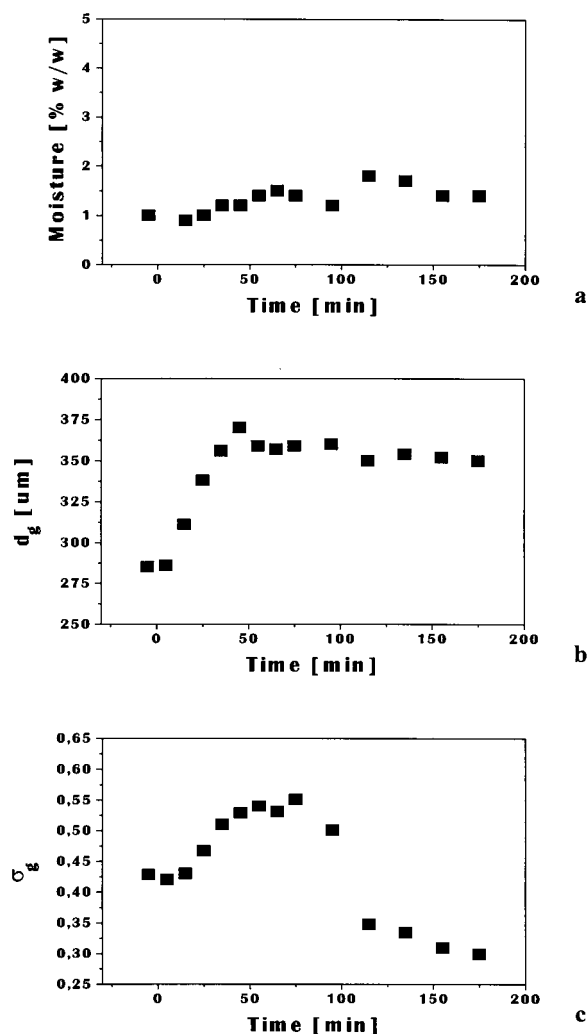


Fig. 9. Product properties produced with the Glatt granulator. (a) Residual moisture; (b) geometric mean diameter; (c) geometric standard deviation. Operation:  $t < 0$ , pre-granulation;  $t = 0$ , change to continuous mode;  $t = 20$ , reduction in drying air rate in granulation zone from 350  $\text{m}^3/\text{h}$  to 300  $\text{m}^3/\text{h}$ ;  $t = 90$ –100, stepwise reductions in drying air rates in fluidization, agglomeration and drying zones to 280  $\text{m}^3/\text{h}$ .



the process conditions (spraying rate or air volumetric flow rate) to produce predictable changes in granule properties. In further experiments these process conditions could be optimized. The two machines, are, however, considered to be unsuitable for research and development purposes by virtue of their large capacities (45–50 kg). Smaller units would be preferable for this purpose.

## Acknowledgements

We thank Niro in Copenhagen and Glatt in Binzen for allowing us to use their machines for this project.

## References

- [1] M. Scott, H. Liebermann, A. Rankell, J.J. Battista, Continuous production of tablet granulation's in a fluidized bed, *Am. Pharm. Assoc. Sci. Ed.* 53 (1964) 314–319.
- [2] N. Lindberg, Continuous wet granulation, *Manuf. Chem.* 12 (1988) 35–38.
- [3] M. Cliff, Continuous granulation. *Technology Transfer Food-Pharma: Production of Solid Dosage Forms. APV-Course No. 406* (1987).
- [4] M. Bonde, Continuous granulation, in: D. Parikh (Ed.), *Handbook of Pharmaceutical Granulation Technology*, Marcel Dekker, New York, 1997, pp. 369–388.
- [5] W. Altensmidt, Where and when is continuous production useful? *Technology Transfer Food-Pharma: Production of Solid Dosage Forms. APV-Course No. 406* (1987).
- [6] G. Körblein, Continuous drying of pharmaceutical granules. *Technology Transfer Food-Pharma. Production of Solid Dosage Forms. APV-Course No. 406* (1987).
- [7] G. Peck, N. Anderson, G. Banker, Principles of improved tablet production system design, in: H. Lieberman, L. Lachmann, J. Schwartz (Eds.), *Pharmaceutical Dosage Forms*, 3, Marcel Dekker, New York, 1990, pp. 1–76.
- [8] Werani, Comparison of batch wise and continuous granulation processes. *APV-Course No. 519* (in German), S. 185 (1990).
- [9] A. Schade, H. Leuenberger, Production of pharmaceutical granules in a combined wet-granulation and multi-chamber fluidized-bed process (in German), *Chem. Ing. Tech.* 64 (1992) 1016–1018.
- [10] R. Hajdu, Z. Ormos, J. Hung, Studies on granulation in fluidized bed, Establishment of steady-state operation conditions in a continuously operated single cell apparatus, *Ind. Chem.* 12 (1984) 333–340.
- [11] A. Grove, Fluidized-bed granulation, in: K. Kadam (Ed.), *Granulation Technology for Bioproducts*, CRC Press, Boston, 1991, pp. 29–70.
- [12] Z. Ormos, Granulation and coating, in: D. Chulia, M. Deleuil, Y. Pourcelot (Eds.), *Handbook of Powder Technology*, 9, Elsevier, Amsterdam, 1994, pp. 359–376.
- [13] M. Bonde, Continuous granulation, in: D. Parikh (Ed.), *Handbook of Pharmaceutical Granulation Technology*, Marcel Dekker, New York, 1998, pp. 369–387.
- [14] Contipharma, *Manufacturer's Information Sheets. Niro A/S-Aeromatic/Fielder, Soeborg, Denmark.*
- [15] D. Parikh, J. Bonck, Batch fluid ged granulation, in: D. Parikh (Ed.), *Handbook of Pharmaceutical Granulation Technology*, Marcel Dekker, New York, 1997, pp. 227–302.